Original Article

Correlation between ^{18}F-FDG PET-derived parameters and quantitative pathological characteristics of soft tissue sarcoma

Bo Chen[1], Juan Tao[2], Tong Wu[3], Hongbo Feng[1], Jinghui Xie[1], Lin Zhong[4], Shaowu Wang[5]

[1]Department of Nuclear Medicine, The First Affiliated Hospital of Dalian Medical University, Dalian, China; [2]Department of Pathology, The Second Affiliated Hospital of Dalian Medical University, Dalian, China; [3]Department of Radiation Oncology, The First Affiliated Hospital of Dalian Medical University, Dalian, China; [4]Department of Pathology, The First Affiliated Hospital of Dalian Medical University, Dalian, China; [5]Department of Radiology, The Second Affiliated Hospital of Dalian Medical University, Dalian, China

Contributions: (I) Conception and design: S Wang; (II) Administrative support: S Wang, B Chen; (III) Provision of study materials or patients: B Chen, J Tao; (IV) Collection and assembly of data: B Chen, T Wu, H Feng; (V) Data analysis and interpretation: B Chen, J Tao, J Xie, L Zhong; (VI) Manuscript writing: All authors; (VII) Final approval of manuscript: All authors.

Correspondence to: Shaowu Wang, PhD. Department of Radiology, The Second Affiliated Hospital of Dalian Medical University, Shahekou district, Zhongshan Road, No. 467, Dalian 116027, China. Email: wsw_2018@163.com.

Background: ^{18}F-fluorodeoxyglucose (^{18}F-FDG) positron emission tomography (PET) has been widely used for evaluating patients with soft tissue sarcoma (STS). However, uncertainties and overlap among individuals may be observed, and the relevance of these findings remains to be further explored. The present study was aimed at investigating the correlation between PET metabolic parameters and quantitative pathological characteristics in STS.

Methods: We retrospectively collected 39 patients with STS who underwent ^{18}F-FDG PET/computed tomography (CT) examination before treatment. Metabolic parameters including the maximum standardized uptake value (SUVmax), metabolic tumor volume (MTV), total lesion glycolysis (TLG), and intratumoral FDG uptake heterogeneity (IFH) were measured. Histological grading was performed according to the French Federation of Cancer Centers grading system. Continuous staining of tissue sections and digital quantitative analysis methods were used, the characteristics of tumor nucleated cells were observed through hematoxylin-eosin staining, and the expression of CD163, CD68, CD8, and CD4 in tumor tissues was determined by immunohistochemistry (IHC), then the correlation between FDG metabolic parameters and the above quantitative pathological characteristics in patients with STS were evaluated.

Results: The SUV_{max} of ^{18}F-FDG PET/CT in STS was positively correlated with the total nuclear area (r=0.355, P=0.027). SUV_{max} was also positively correlated with the expression levels of CD163, CD68, CD8, and CD4 (r=0.582, 0.485, 0.343, and 0.324, with P<0.001, 0.002, 0.032, and 0.044, respectively), but was not significantly correlated with cell count and mean nuclear area (all P>0.05). However, MTV, TLG, and IFH were not significantly correlated with the above quantitative pathological characteristics. Further multivariate logistic regression analysis indicated that only CD163 expression and histological grade were independently correlated with SUV_{max}. Moreover, SUV_{max} remained positively correlated with CD163 expression in the low-grade STS (r=0.820, P=0.001) and high-grade STS groups (r=0.430, P=0.028).

Conclusions: ^{18}F-FDG uptake was positively correlated with the quantitative pathological features of soft tissue tumors. SUV_{max} may be a meaningful method reflecting the level of M2 macrophage infiltration and may provide additional valuable information for preclinical evaluation of STS.

Keywords: Soft tissue sarcoma (STS); ^{18}F-fluorodeoxyglucose (^{18}F-FDG); positron emission tomography (PET); metabolic parameter; pathological characteristic

Submitted Mar 31, 2023. Accepted for publication Sep 06, 2023. Published online Oct 19, 2023.
doi: 10.21037/qims-23-412
View this article at: https://dx.doi.org/10.21037/qims-23-412

Introduction

Soft tissue sarcoma (STS) is a malignant tumor of mesenchymal origin that exists in almost all parts of the body. Its biological characteristics include aggressiveness, high recurrence, and metastatic potential (1,2). In recent years, despite great progress in multidisciplinary treatment, the survival outcomes of patients with STS have not significantly improved, thus severely endangering human health (2-4). Hence, a dire need exists to explore new methods to improve STS management strategies.

Some researchers have found that malignant tumors are mixed complexes composed of tumor cells and their tumor microenvironment (5-8), which promote the occurrence and development of tumors under their combined action. STS, a group of highly heterogeneous malignant tumors, shows diverse morphologic manifestations in their tumor tissues. This diversity has been found to be an important cause of heterogeneity in STS biological behavior, thus complicating the selection of their clinical management strategies. In addition, in STS, as in most solid tumors, the tumor stroma is composed primarily of high-density tumor-associated macrophage (TAM) and tumor infiltrating lymphocyte (TIL). Macrophages, the main components of the innate immune system, account for approximately 30–50% of the tumor tissue (6). M2 TAM have been shown to have biological effects that promote STS cell growth and metastasis, stimulate angiogenesis, modulate immunosuppression, and mediate antitumor activity of chemoradiation (7,8). Cytotoxic T lymphocytes CD8 directly kill tumor cells with tumor-associated antigens, and CD4 is a donor receptor that enables helper T cells to recognize antigens and participates in signal transduction. Both these functions are essential for adaptive immune responses in tumors, and are tightly associated with STS prognosis and the effectiveness of anti-immunotherapy (7,8).

The classical molecular imaging technique of ^{18}F-fluorodeoxyglucose (^{18}F-FDG) positron emission tomography/computed tomography (PET/CT) has been widely used in the evaluation of STS, and can also serve as a supplement to traditional imaging methods (9). Previous studies have demonstrated the importance of metabolic parameters of FDG PET in assessing the therapeutic response, prognosis, and histological grading of patients with STS (10-12). However, in some studies, standardized uptake value (SUV) in patients with STS with the French Federation of Cancer Centres (FNCLCC) II and III was found to have approximate median (12). In addition, FDG uptake can greatly vary among individuals, even those with the same histologic grading level. The intrinsic reasons underlying this association must be further explored.

Consequently, the present study retrospectively collected a group of patients who underwent ^{18}F-FDG PET/CT and had pathologically confirmed STS. Continuous sections of tumor tissues were stained with HE and IHC, digitally processed, and to perform quantitative analysis of both tumor nucleated cell characteristics and tumor immune cell infiltration. The correlations between FDG metabolic parameters and these quantitative pathological characteristics were further investigated. Our aim was to provide new ideas for exploring STS management strategies based on PET/CT. We present this article in accordance with the STROBE reporting checklist (available at https://qims.amegroups.com/article/view/10.21037/qims-23-412/rc).

Methods

Patient selection and data management

The present study was performed in accordance with the Declaration of Helsinki (as revised in 2013) and was approved by the Institutional Ethics Committee of The First Hospital of Dalian Medical University (No. PJ-KS-KY-2021-249). The requirement for individual consent for this retrospective analysis was waived. We retrospectively screened 39 patients with STS who underwent ^{18}F-FDG PET/CT examination before treatment, from December 2012 to October 2021. The specific enrollment process is shown in *Figure 1*. The cohort consisted of 19 men and 20 women with a median age of 59.0 (range, 32.0–84.0) years.

^{18}F-FDG PET/CT imaging protocol and image analysis

All patients were required to fast for more than 6 hours. Their blood glucose was less than 10.0 mmol/L, and ^{18}F-FDG was injected intravenously at 5.55 MBq/kg for approximately 60 min before machine collection. The same

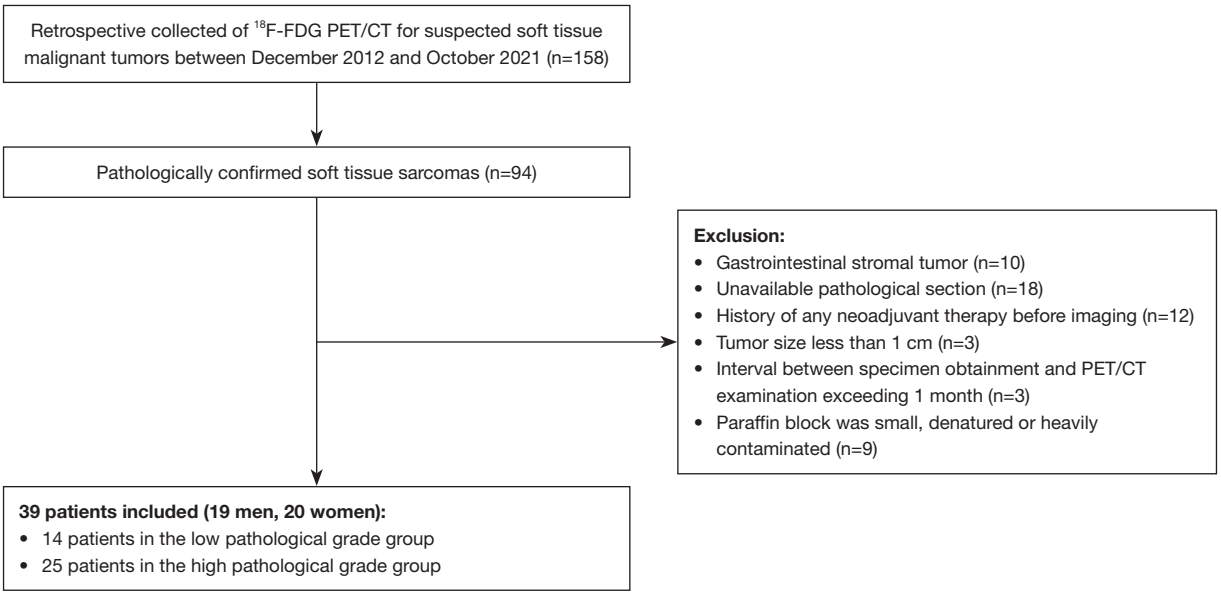

Figure 1 Flowchart depicting study population selection. ^{18}F-FDG, ^{18}F-fluorodeoxyglucose; PET/CT, positron emission tomography/computerized tomography.

PET scanner (Biograph True-Point Row 64, Siemens, Erlangen, Germany) was used for all patients. CT and PET images were collected successively, with a matrix of 168×168, tube voltage of 120 kV, tube current for care-dose automatic adjustment, range of 60–80 mAs, and pitch of 0.8. The PET scans used 3-dimensional acquisition mode, 1.5 min/bed, with an axial field of view of 500 mm and a layer thickness of 5 mm. The OSEM and PSF reconstruction method was used with three iterations, 21 subsets, and a Gaussian filter half height width of 4 mm. CT was used for attenuation correction of the PET data set.

The image data were processed on a standard MMWP workstation in TureD software (Siemens Healthcare). First, the circular ROI was manually selected on the maximum cross-section of the tumor; a spherical volume of interest (VOI) was automatically generated, and finally, manual fine-tuning was performed to ensure that the VOI sufficiently covered the tumor target in three planes (coronal, sagittal, and transverse). The maximum standardized uptake value (SUV_{max}) and mean maximal standardized uptake value (SUV_{mean}) were automatically obtained. Metabolic tumor volume (MTV) was defined as the total volume of voxels within the VOI, which was higher than SUV =2.5 (13). Total lesion glycolysis (TLG) was obtained by multiplication of MTV and SUV_{mean}. Additionally, intratumoral FDG uptake heterogeneity (IFH) was calculated on the basis of the derivative of the metabolic volume/threshold (dV/dT); according to previous studies, the volume-based threshold was adjusted to 30–70% (14). Two experienced radiologists independently performed double-blinded readings and measurements. Consistency analysis was performed on the determined measurements, and the average value was finally used in statistical analysis.

Histopathologic staining and analysis

Two pathologists who were blinded to the ^{18}F-FDG PET/CT results re-interpreted the histological subtypes of the enrolled patients according to the 2020 WHO guidelines for the classification of soft tissue tumors. The pathological subtypes included liposarcoma (n=4), fibrosarcoma (n=6), synovia sarcoma (n=6), undifferentiated sarcoma (n=8), leiomyosarcoma (n=7), angiosarcoma (n=5), rhabdosarcoma (n=1), and extrasolar-skeletal muscle sarcoma (n=2). STS were histopathologically classified as grade I, II, and III according to the FNCLCC grading system (15): FNCLCC I (n=6), FNCLCC II (n=8), FNCLCC III (n=25). According to previous study (16), the enrolled population with grade I and II STS was further defined as the low-grade group (n=14), and the population with grade III STS was defined as the high-grade group (n=25), as summarized in *Table 1*.

Tumor sample staining

Two pathologists selected the tissue paraffin blocks

Table 1 Corresponding table for histopathological types and histological grading of the enrolled patients

Histopathological type	Total	FNCLCC		
		I	II	III
Liposarcoma	4	1	0	3
Fibrosarcoma	6	1	2	3
Synovia sarcoma	6	0	2	4
Undifferentiated sarcoma	8	0	0	8
Leiomyosarcoma	7	3	0	4
Angiosarcoma	5	1	2	2
Rhabdosarcoma	1	0	0	1
Extrasolar-skeletal muscle sarcoma	2	0	2	0
Total	39	6	8	25

FNCLCC, French Federation of Cancer Centers.

corresponding to the sections with the most tumor histopathologic characteristics and performed continuous sampling to prepare multiple 4-μm-thick tissue sections. Tumor cell characteristics were obtained from hematoxylin-eosin-stained tumor sections through routine histological assessment. Immunohistochemistry (IHC) was performed with the indirect streptavidin-biotin method. Briefly, the operation steps were as follows. Tissue white slices were baked, degreased, and rehydrated, then placed in citric acid repair solution for antigen repair. Different primary antibody dilutions were added. After incubation for 60 min in a 37 ℃ incubator, secondary antibodies were added and incubated in parallel at room temperature. This was followed by re-staining with DAB immunostaining agent, hematoxylin staining, dehydration with a graded alcohol series, and neutral resin sealing. With respect to a spleen tissue positive control during the same period, brownish-yellow staining of cytoplasm and/or membrane of tumor cells in tumor tissue sections was defined as positive staining.

Tumor sample analysis

Observations and digital image capture were performed through investigational light microscopy (Leica Laboratories, Wetzlar, Germany) with the assistance of two experienced pathologists. The most densely packed area of tumor cells, according to hematoxylin and eosin (H&E) staining, and the most representative areas of IHC cell staining were selected under low magnification (×40). Subsequently, digital images were acquired under high magnification (×400), in five randomly selected non-overlapping areas. Quantitative analysis was performed in Fiji ImageJ software 1.48v as previously described (17,18). Analytical values were obtained for tumor cell characteristics, including cell counts, total nuclear area, and mean nuclear area (*Figure 2*). The total protein expression of each immune cell marker stain was quantified as the integrated optical density (IOD), and the average values for five images were used in the analysis (*Figure 3*).

Statistical analysis

IBM SPSS 26.0 software was used. The Kolmogorov-Smirnov method was used to test the normality of continuous variables. Statistical descriptions of continuous variables with a non-normal distribution are described by median (Q1–Q3). The correlation test of two factors was performed with Spearman's correlation analysis by using the correlation coefficient. Two-group comparisons of continuous variables were assessed with Mann-Whitney *U* tests. Multiple linear regression analysis was used to evaluate factors independently associated with metabolic parameters. The intra-group correlation coefficient test was used for consistency analysis. A probability (P) <0.05 was considered statistically significant.

Results

^{18}F-FDG PET-derived parameters in patients with STS

The metabolic parameters of PET/CT in patients

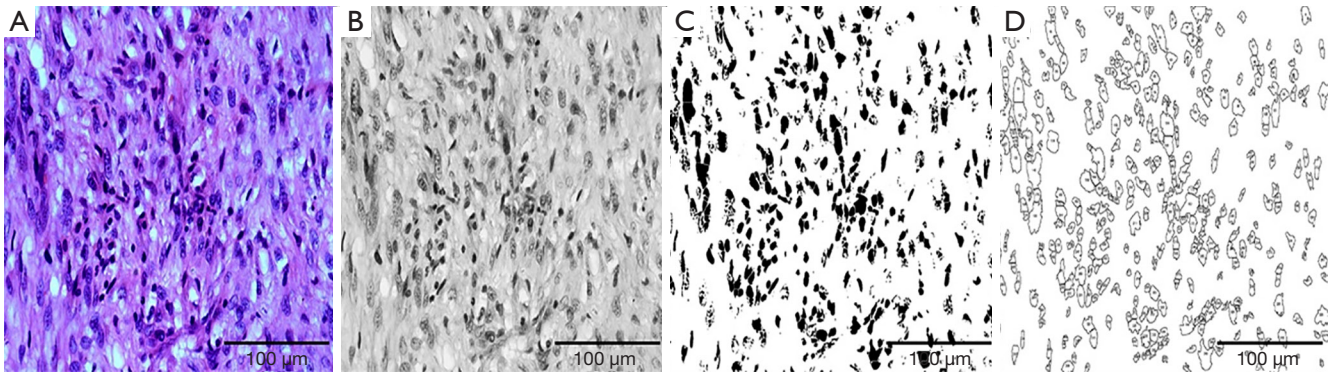

Figure 2 Schematic diagram of digital quantitative analysis of H&E staining images. (A) Original format (Tiff) pathological images of H&E staining taken with a microscope and camera diagnostic instrument; (B) conversion of H&E stained pathological images to Bit8 format; (C) conversion to black and white binarized images, by setting image thresholds and separating cells with the watershed method; (D) selection of the threshold values according to the set image analysis section, to obtain quantitative parameter values. H&E, hematoxylin and eosin.

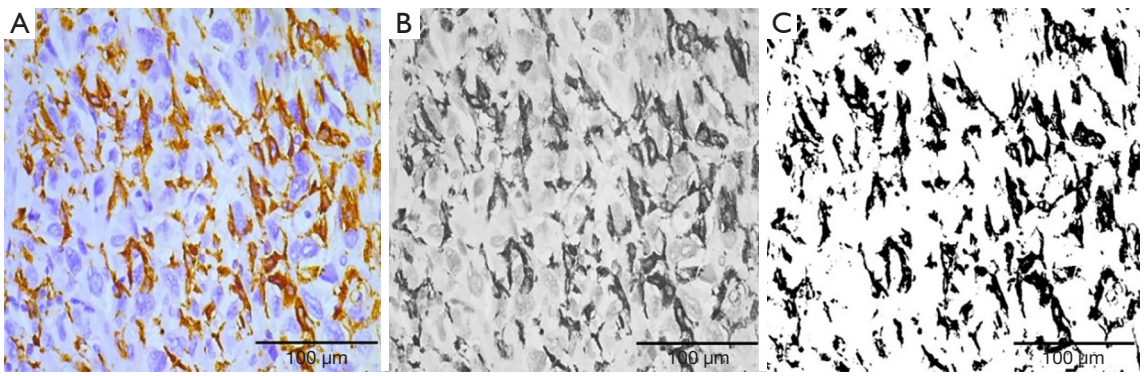

Figure 3 Schematic diagram of digital quantitative analysis of immunohistochemical staining images. (A) IHC image in its original format (Tiff), taken with a microscope and camera diagnostic instrument; (B) conversion to Bit8 format; (C) conversion to a binarized black and white image by setting the image threshold for quantitative analysis and obtaining quantitative parameter values. IHC, immunohistochemistry.

with STS were summarized in *Table 2*. Each metabolic parameter in the high-grade group was higher than that in the low-grade group. Moreover, heterogeneity in metabolic parameters was observed among patients with the same pathological type.

Quantitative pathological characteristics of patients with STS

The quantitative pathological characteristics of patients with STS were summarized. The quantitative values of tumor nucleated cell characteristics analyzed in patients, as determined by HE staining, included cell count, total nuclear area, and mean nuclear area, with median of 470 (Q1–Q3: 316–569), 13,731.61 (Q1–Q3: 10,463.36–17,710.37), and 30.51 (Q1–Q3: 25.21–36.64), respectively. Heterogeneity in cell counts, total nuclear area, and mean nuclear area was observed among individuals.

Immunohistochemical staining for CD163, CD68, CD8, and CD4 appeared as brown or brownish-yellow cytoplasm and/or membranes of tumor cells, respectively. The IODs of these immune markers were 43,493.03 (Q1–Q3: 11,570.00–18,069.51), 12,106.21 (Q1–Q3: 2,804.34–34,703.97), 6,384.48 (Q1–Q3: 3,180.59–16,727.14), and 8,850.24 (Q1–Q3: 4,689.25–24,689.3), respectively (*Table 3*). We also observed heterogeneous expression of these tumor-infiltrating immune cells (TIICs) (*Figure 4*). Among them, TAM (CD163 and CD68) had more intense staining than

Table 2 Summary of FDG-based metabolic parameters in patients with STS

Metabolic parameters	Total (n=39)	FNCLCC grouping	
		Low-grade group (n=14)	High-grade group (n=25)
SUV_{max}	12.80 (7.69–18.60)	8.60 (4.90–11.35)	14.20 (9.83–20.15)
MTV, cm^3	57.87 (11.2–138.38)	9.75 (3.12–76.29)	97.79 (32.63–201.26)
TLG	219.43 (42.01–900.14)	37.46 (10.05–335.92)	433.72 (166.92–1,145.13)
IFH	0.92 (0.35–2.03)	0.39 (0.19–0.92)	1.24 (0.63–3.29)

Statistical description by median (Q1–Q3). FDG, fluorodeoxyglucose; STS, soft tissue sarcoma; FNCLCC, French Federation of Cancer Centers; SUV_{max}, maximum standardized uptake value; MTV, metabolic tumor volume; TLG, total lesion glycolysis; IFH, intertumoral FDG uptake heterogeneity.

Table 3 Summary of the quantitative pathological characteristics in patients with STS

Pathological characteristics	Total (n=39)	FNCLCC Grouping	
		Low-grade group (n=14)	High-grade group (n=25)
Cell count	470 (316–569)	487.8 (304–717.9)	457.6 (345.9–548.35)
Total nuclear area	13,731.61 (10,463.36–17,710.37)	12,484.43 (8,573.66–14,552.81)	14,454.61 (12,851.46–18,363.69)
Mean nuclear area	30.51 (25.21–36.64)	25.56 (21.31–28.1)	31.4 (27.69–37.45)
$CD163^+$ IOD	43,493.03 (11,570.00–18,069.51)	14,610.18 (7,855.08–47,464.03)	28,769.51 (13,709.18–73,075.97)
$CD68^+$ IOD	12,106.21 (2,804.34–34,703.97)	11,226.06 (3,744.11–25,239.30)	12,703.74 (3,692.15–35,727.09)
$CD8^+$ IOD	6,384.48 (3,180.59–16,727.14)	3,281.45 (2,528.79–9,891.13)	8,703.94 (4,036.73–17,808.18)
$CD4^+$ IOD	8,850.24 (4,689.25–24,689.3)	7,291.78 (3,835.78–16,309.04)	10,255.3 (5,495.27–22,603.12)

Statistical description by median (Q1–Q3). STS, soft tissue sarcoma; FNCLCC, French Federation of Cancer Centers; IOD, integrated optical density.

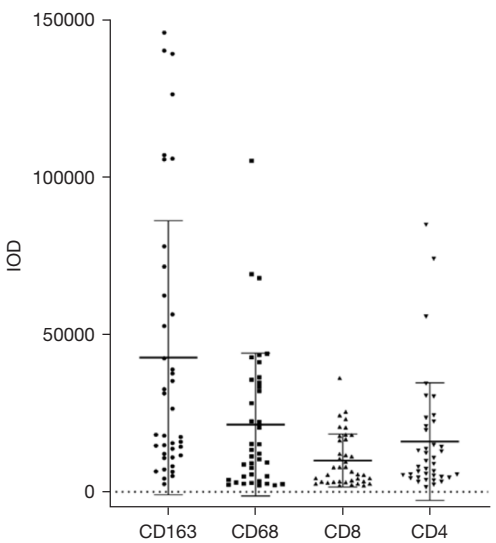

Figure 4 Scatterplots of the expression levels of each infiltrating immune cell in tumor tissues from patients with STS. IOD, integrated optical density; STS, soft tissue sarcoma.

TIL (CD8 and CD4), and CD163 had the highest intensity.

Correlation between the ^{18}F-FDG PET-derived parameters and quantitative pathologic characteristics in patients with STS

The metabolic parameter SUV_{max} of PET in patients in the enrolled cohort was positively correlated with the total nuclear area of tumor cells (r=0.355, P=0.027). SUV_{max} was also positively correlated with the expression of CD163, CD68, CD8, and CD4 in tumor tissues (r=0.582, 0.485, 0.343, and 0.324, all P<0.05). The correlation between SUV_{max} and CD163 was more significant than the correlations with the other immune markers. However, SUV_{max} was not significantly correlated with cell count and mean nuclear area, and the MTV, TLG, and IFH values were not significantly correlated with the cell count, total nuclear area, and mean nuclear area, respectively (all P>0.05). Moreover, the MTV, TLG, and IFH values were

Table 4 Associations between FDG-based metabolic parameters of STS with quantitative pathologic characteristics

Metabolic parameters	Quantitative pathologic characteristics						
	Cell counts	Total nuclear area	Mean nuclear area	CD163	CD68	CD8	CD4
SUV_{max}							
r	–0.013	0.355	0.153	0.582	0.485	0.343	0.324
P	0.935	0.027*	0.352	0.000*	0.002*	0.032*	0.044*
MTV, cm^3							
r	–0.210	0.015	0.109	0.196	0.213	0.291	0.241
P	0.200	0.929	0.508	0.232	0.193	0.072	0.139
TLG							
r	–0.188	0.095	0.135	–0.283	0.278	0.287	0.283
P	0.251	0.565	0.413	0.081	0.087	0.052	0.081
IFH							
r	–0.068	0.143	0.110	–0.091	–0.003	0.162	0.022
P	0.681	0.385	0.506	0.581	0.985	0.323	0.896

*, P value was statistically significant. FDG, fluorodeoxyglucose; STS, soft tissue sarcoma; SUV_{max}, maximum standardized uptake value; r, correlation coefficient; MTV, metabolic tumor volume; TLG, total lesion glycolysis; IFH, intertumoral FDG uptake heterogeneity.

Table 5 Multiple linear regression analysis of the associations between SUV_{max} on FDG PET and pathologic characteristics

Variables	Multiple analysis		
	β	*t* value	P value
Histological grading	0.285	2.049	0.048*
Total nuclear area	0.177	1.349	0.187
$CD163^+$ IOD	0.616	3.007	0.005*
$CD8^+$ IOD	0.212	1.503	0.142
$CD4^+$ IOD	–0.333	–1.592	0.121

*, P value was statistically significant. FDG, fluorodeoxyglucose; PET, positron emission tomography; SUV_{max}, maximum standardized uptake value; IOD, integrated optical density.

not significantly correlated with the expression levels of the above TIICs (*Table 4*).

Multiple linear regression analysis of the correlation between SUVmax and quantitative pathologic characteristics in patients with STS

With SUV_{max} as the dependent variable, according to the collinearity test results, the collinearity factor CD68 was first removed; finally, histological grade, the total nuclear area of tumor cells, and the expression of CD163, CD8, and CD4 were included as independent variables in multiple linear regression analysis. Histological grade and CD163 expression of STS were the independent factors associated with SUV_{max} (*Table 5*), and the standardized coefficient β was 0.285 and 0.616, respectively (P=0.048 and 0.005). A positive correlation between SUVmax and CD163 expression was observed in both the low-grade group (n=14, r=0.820, P=0.001) and high-grade group (n=25, r=0.430, P=0.028), as presented as a scatter plot in *Figure 5*. The representative cases are shown in *Figures 6*,*7*.

Discussion

Otto Warburg *et al.*, as early as 1920s, indicated that in malignant cells, glycolytic pathways are preferred for metabolic energy supply, even when oxygen is sufficient, and high rates of glucose-metabolism are observed, i.e., the "Warburg Effect" (19). This effect also provides the basis for ^{18}F-FDG PET for tumor imaging using radiotracers to "illuminate" malignant cells on the basis of glucose metabolism in cancer cells (20). According to current understanding, tumors are not considered masses formed by the accumulation of tumor cells present in only specific organs or sites, except in heterogeneous malignant tumor cells, TIIC in the tumor stroma are understood to account

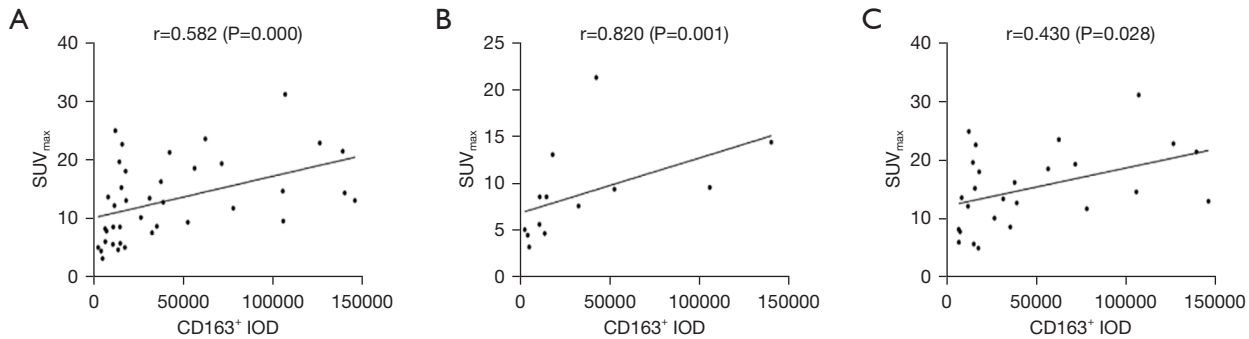

Figure 5 Scatterplot of the correlation between SUV_{max} on FDG PET and CD163 expression in patients with STS. (A-C) Scatter plots of the correlation between SUV_{max} and CD163 expression in the overall cohort (n=39, r=0.582, P=0.000), in the low-grade group (n=14, r=0.820, P=0.001), and in the high-grade group (n=25, r=0.430, P=0.028), respectively. SUV_{max}, maximum standardized uptake value; IOD, integrated optical density; FDG, fluorodeoxyglucose; PET, positron emission tomography; STS, soft tissue sarcoma.

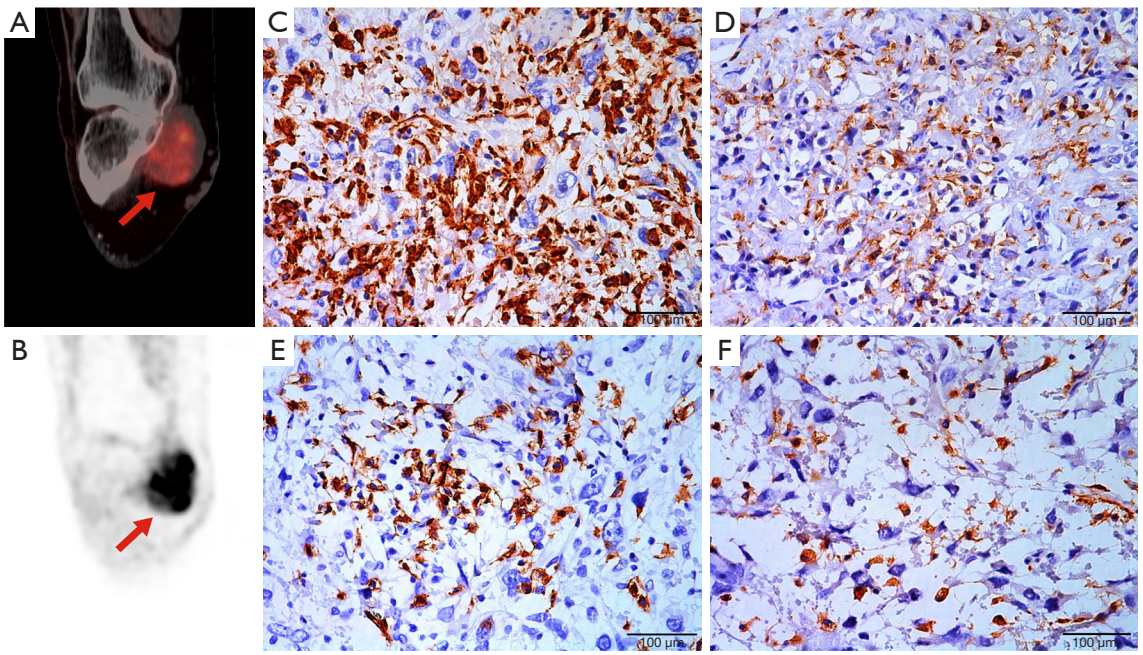

Figure 6 Representative Case 1. A 66-year-old woman with postoperative pathology of undifferentiated sarcoma in the anterior part of the right knee joint (FNCLCC III). (A) PET/CT fusion images. (B) PET, sagittal plane. As indicated by the red arrows, the density of the mass was slightly low and uneven, and showed strong and heterogeneous FDG uptake. Tumor size =5.9 cm, SUV_{max} =13.1, MTV =92.85 cm^3, TLG =439.18, IFH =0.98. (C-F) Photomicrographs (IHC, ×400) for CD163, CD68, CD8, and CD4, with IOD values of 145,793.77, 43,432.39, 17,722.21, and 73,969.21, respectively. FNCLCC, the French Federation of Cancer Centres; PET/CT, positron emission tomography/computed tomography; FDG, fluorodeoxyglucose; SUVmax, maximum standardized uptake value; MTV, metabolic tumor volume; TLG, total lesion glycolysis; IFH, intertumoral FDG uptake heterogeneity; IHC, immunohistochemistry; IOD, integrated optical density.

for a large proportion of the tumor mass (21). In the present study, we performed the first quantitative digitized analysis of the characteristics of tumor nucleated cells and tumor stromal immune cell infiltrates in STS patient tissues. Further analysis indicated that SUV_{max} in patients with STS was associated with these described histopathological characteristics, thus providing a new direction and a preliminary theoretical basis for determining the

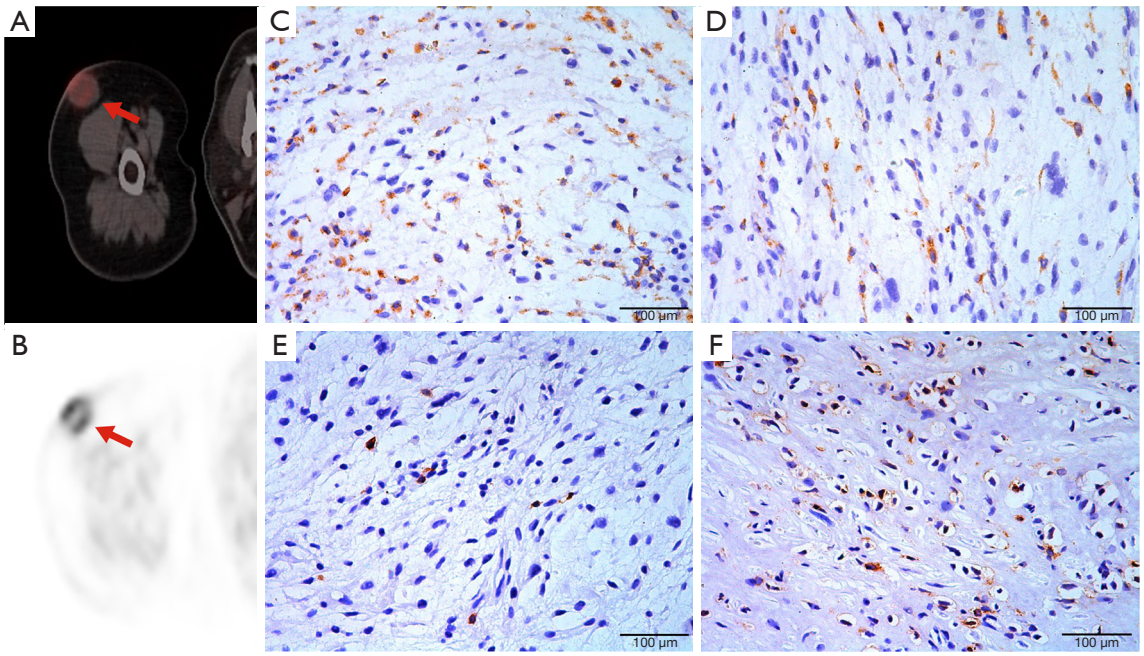

Figure 7 Representative Case 2. A 68-year-old woman with postoperative pathology of fibrosarcoma in the right arm (FNCLCC I). (A) PET/CT fusion images. (B) PET, sagittal plane. As indicated by the red arrows, a slightly dense mass, seen on the right forearm, showed diffuse and slightly elevated FDG metabolism. Tumor size =2.3 cm, SUV_{max} =4.7, MTV =4.50 cm^3, TLG =14.9, IFH =0.16. (C-F) Photomicrographs (IHC, ×400) for CD163, CD68, CD8, and CD4, with IOD values of 13,644.03, 11,226.06, 11,999.27, and 33,089.77, respectively. FNCLCC, the French Federation of Cancer Centres; FDG, fluorodeoxyglucose; SUV_{max}, maximum standardized uptake value; MTV, metabolic tumor volume; TLG, total lesion glycolysis; IFH, intertumoral FDG uptake heterogeneity; IHC, immunohistochemistry; IOD, integrated optical density.

heterogeneity of the biological behavior of STS according to ^{18}F-FDG PET.

Like most other solid tumors, in STS, the tumor stroma is dominated by high density of TAM and TIL (7). TAM are the most abundant tumor stromal cells involved in the host immune system of malignant tumors (22). Previous studies have shown that most macrophages in the STS tumor microenvironment have an M2 macrophage phenotype and high CD163 expression (23). M2 macrophages play crucial roles in promoting STS tumor cell growth and metastasis, stimulating angiogenesis, mediating immunosuppression, and limiting the antitumor activity of conventional chemoradiotherapy, thus revealing that tumors with greater M2 macrophage infiltration have poor prognosis (24,25). Typically, the expression of TIIC in the target type can be identified by pathological examination, but this method is limited by preoperative small sample sampling error and a postoperative pathological lag, and cannot dynamically reflect the global immune cell distribution of the tumor. Therefore, if noninvasive methods can be used to identify and assess levels of important immune cells infiltrating the tumor stroma before treatment, they might aid in predicting prognosis and providing preclinical evidence for screening dominant groups for individualized treatment. Nevertheless, to date, PET-based targeting of the tumor immune microenvironment has not been incorporated into routine clinical practice; therefore, exploring alternative conventional imaging methods is a meaningful research direction.

Hyperglycemia is one of the top ten features of malignant tumors, and FDG uptake detected by PET imaging is a good indicator of its aerobic glycolysis. We hypothesized that STS is a highly heterogeneous malignancy. In addition to tumor cells, the TIIC in tumor stroma may also be associated with altered uptake of ^{18}F-FDG, thus resulting in different PET visual images. A recent cytological experimental study by Reinfeld *et al.* has shown that macrophages have higher glucose uptake capacity than rectal and breast cancer cells, and other immune cells (26). Another study has found that

macrophages promote glycolysis by secreting TNFα in NCLCC (27). Therefore, we speculated that observation of differences in ^{18}F-FDG PET imaging might enable the assessment of the heterogeneity of pathological features *in vivo* among patients with STS.

Given the diversity of STS histological types, tumors' nucleated cell features and immune cell infiltration were simultaneously observed in the present study. We observed varying degrees of TAM and TIL in the tumor stroma in patients with STS. The number of TAM exceeded that of TIL, and CD163 was more abundant than CD68, in agreement with previous findings (28). These results might have been because, during the development of malignancy, as tumor tissue cell metabolism is reprogrammed, the TME transforms into a microenvironment conducive to tumor growth. The results of the present study suggest that the SUV_{max} of STS is positively correlated with the total area of nucleated cells in the tumor, similar to findings in head and neck squamous cell carcinoma and cervical cancer (29,30). We also observed that patients with higher SUV_{max} had more TAM and TIL in the tumor stroma. SUV_{max} was more strongly correlated with $CD163^+$ TAM than $CD68^+$ TAM, $CD8^+$ TIL, and $CD4^+$ TIL, and higher than the total area of tumor nucleated cells. In multivariate analysis corrected for total tumor nucleated cell area and other immune cell infiltration, SUV_{max} remained associated with CD163.

As compared with previous studies (18,31,32), most existing studies have observed correlations between the pathological features of one of the above tumors and imaging markers, ignoring the co-existence of tumor cells and the tumor immune cells as a whole. Few reports have described the correlation in STS. Only a study by Skubitz *et al.* (22) in 31 patients with STS has found that SUV_{max} is positively correlated with CD68 expression, but that CD68, a pan-TAM marker, is less clinically meaningful than M2 TAM. In this study, associated tissue sections staining and digital quantification methods were used to analyze the tumor nucleated cell characteristics of STS in H&E stained tissue and tumor immune cell infiltration levels in IHC stained tissue, thus overcoming subjective inter-observer errors, decreasing the shortcomings of including patients with diverse histological types in the cohort, and improving the reliability of the results. According to the results of the present study, higher SUV_{max} within the same histological grade group was associated with greater infiltration of M2 TAM within the tumor stroma, thus suggesting that higher SUV_{max} might predict poor prognosis and potential benefits of immunotherapy. However, the results of this study indicated only a moderate correlation between SUV_{max} and immune markers. To better apply to clinical practice, future studies with large sample sizes remain needed.

In addition, according to the data from this study, no correlations were found between SUV_{max} on FDG PET and the tumor nucleated cell count and mean nuclear area; moreover, no correlation was found between other metabolic parameters (MTV, TLG, and IFH) and tumor nucleated cell characteristics, as well as the amount of tumor immune cell infiltration. These findings might have been because FDG uptake in malignant cells is related primarily to the proportion of tumor cellularity, but the correlation between FDG uptake and cell density is not significant. However, the biological effects caused by the pathological features of tumor cells, particularly the heterogeneous changes at the TIIC level, span the entire process of tumor occurrence and development (24); consequently, no significant correlation with tumor diameter or volume/size was observed. Recently, IFH values as a parameter of heterogeneity in the distribution of FDG uptake have been proposed by scholars and reported to be predictive of tumor biomarkers in some tumor types (33,34). However, this study did not find an association between IFH and pathological characteristics of STS, possibly because of the small number of enrolled samples or population differences in this cohort. The sample size will be expanded to further perform continuous observation.

Our study has several limitations. First, ^{18}F-FDG PET/CT was performed predominantly before surgery in patients with high grade STS, because clinicians believe that these patients are relatively likely to develop distant metastases. This aspect inevitably led to a smaller sample size in the low-grade group. Second, because of the low morbidity of STS, the sample size was limited, and a single pathological type could not be explored separately. Third, because this was a retrospective study, the choice of radiographically delineated ROIs with pathological tissue sections was inevitably influenced by tumor heterogeneity. Finally, this study describes only preliminary results; whether these immune cells act directly on ^{18}F-FDG uptake and what mechanism might underlie this association remain unclear. A large sample prospective study design and cytological experimental validation will be pursued in our future research.

Conclusions

In conclusion, this study found that FDG uptake may

meaningfully reflect the heterogeneity of histopathological features of STSs, and may be considered a surrogate marker for determining the heterogeneity in biological behavior in patients with STS.

Acknowledgments

The authors would like to express their gratitude to colleagues for helping in patient collection.
Funding: This work was supported by grants from the National Natural Science Foundation of China (No. 82271975) and Medical Scientific Research Program of Dalian (No. 2212010).

Footnote

Reporting Checklist: The authors have completed the STROBE reporting checklist. Available at https://qims.amegroups.com/article/view/10.21037/qims-23-412/rc

Conflicts of Interest: All authors have completed the ICMJE uniform disclosure form (available at https://qims.amegroups.com/article/view/10.21037/qims-23-412/coif). The authors have no conflicts of interest to declare.

Ethical Statement: The authors are accountable for all aspects of the work in ensuring that questions related to the accuracy or integrity of any part of the work are appropriately investigated and resolved. The present study was performed in accordance with the Declaration of Helsinki (as revised in 2013) and approved by the Institutional Ethics Committee of The First Hospital of Dalian Medical University (No. PJ-KS-KY-2021-249), individual consent for this retrospective analysis was waived.

References

1. Rothermundt C, Fischer GF, Bauer S, et al. Pre- and Postoperative Chemotherapy in Localized Extremity Soft Tissue Sarcoma: A European Organization for Research and Treatment of Cancer Expert Survey. Oncologist 2018;23:461-7.
2. Hui JY. Epidemiology and Etiology of Sarcomas. Surg Clin North Am 2016;96:901-14.
3. Ezuddin NS, Pretell-Mazzini J, Yechieli RL, et al. Local recurrence of soft-tissue sarcoma: issues in imaging surveillance strategy. Skeletal Radiol 2018;47:1595-606.
4. In GK, Hu JS, Tseng WW. Treatment of advanced, metastatic soft tissue sarcoma: latest evidence and clinical considerations. Ther Adv Med Oncol 2017;9:533-50.
5. Arner EN, Rathmell JC. Metabolic programming and immune suppression in the tumor microenvironment. Cancer Cell 2023;41:421-33.
6. Castaneda CA, Castillo M, Aliaga K, et al. Level of tumor-infiltrating lymphocytes and density of infiltrating immune cells in different malignancies. Biomark Med 2019;13:1481-91.
7. Fujiwara T, Healey J, Ogura K, et al. Role of Tumor-Associated Macrophages in Sarcomas. Cancers (Basel) 2021;13:1086.
8. Ruiz-Mesa C, Goldberg JM, Coronado Munoz AJ, et al. Rhabdomyosarcoma in adults: new perspectives on therapy. Curr Treat Options Oncol 2015;16:27.
9. Blay JY, Hindi N, Bollard J, et al. SELNET clinical practice guidelines for soft tissue sarcoma and GIST. Cancer Treat Rev 2022;102:102312.
10. Annovazzi A, Ferraresi V, Anelli V, Covello R, Vari S, Zoccali C, Biagini R, Sciuto R. [18F]FDG PET/CT quantitative parameters for the prediction of histological response to induction chemotherapy and clinical outcome in patients with localised bone and soft-tissue Ewing sarcoma. Eur Radiol 2021;31:7012-21.
11. Kitao T, Shiga T, Hirata K, et al. Volume-based parameters on FDG PET may predict the proliferative potential of soft-tissue sarcomas. Ann Nucl Med 2019;33:22-31.
12. Zhang Q, Xi Y, Li D, et al. The utility of (18)F-FDG PET and PET/CT in the diagnosis and staging of chondrosarcoma: a meta-analysis. J Orthop Surg Res 2020;15:229.
13. Iwasa H, Nagamachi S, Nakayama S, et al. The reproducibility of MTV and TLG of soft tissue tumors calculated by FDG-PET: Comparison between the lower limit by the fixed value SUV 2.5 and that value by 30% of SUVmax. Jpn J Radiol 2023;41:531-40.
14. Kimura M, Kato I, Ishibashi K, et al. The prognostic significance of intratumoral heterogeneity of 18F-FDG

uptake in patients with oral cavity squamous cell carcinoma. Eur J Radiol 2019;114:99-104.
15. Coindre JM. Grading of soft tissue sarcomas: review and update. Arch Pathol Lab Med 2006;130:1448-53.
16. Sagiyama K, Watanabe Y, Kamei R, et al. Multiparametric voxel-based analyses of standardized uptake values and apparent diffusion coefficients of soft-tissue tumours with a positron emission tomography/magnetic resonance system: Preliminary results. Eur Radiol 2017;27:5024-33.
17. Zhang Y, Li H, Jia Y, et al. Noninvasive Assessment of Carotid Plaques Calcification by (18)F-Sodium Fluoride Accumulation: Correlation with Pathology. J Stroke Cerebrovasc Dis 2018;27:1796-801.
18. Du P, Ma Q, Zhu ZD, et al. Mechanism of Corilagin interference with IL-13/STAT6 signaling pathways in hepatic alternative activation macrophages in schistosomiasis-induced liver fibrosis in mouse model. Eur J Pharmacol 2016;793:119-26.
19. Hardie DG. 100 years of the Warburg effect: a historical perspective. Endocr Relat Cancer 2022;29:T1-13.
20. Sigal IR, Sebro R. Preclinical PET tracers for the evaluation of sarcomas: understanding tumor biology. Am J Nucl Med Mol Imaging 2018;8:428-40.
21. Fendler WP, Chalkidis RP, Ilhan H, et al. Evaluation of several FDG PET parameters for prediction of soft tissue tumour grade at primary diagnosis and recurrence. Eur Radiol 2015;25:2214-21.
22. Skubitz KM, Wilson JD, Cheng EY, et al. Effect of chemotherapy on cancer stem cells and tumor-associated macrophages in a prospective study of preoperative chemotherapy in soft tissue sarcoma. J Transl Med 2019;17:130.
23. Cheng N, Bai X, Shu Y, et al. Targeting tumor-associated macrophages as an antitumor strategy. Biochem Pharmacol 2021;183:114354.
24. Dumars C, Ngyuen JM, Gaultier A, et al. Dysregulation of macrophage polarization is associated with the metastatic process in osteosarcoma. Oncotarget 2016;7:78343-54.
25. Cassetta L, Pollard JW. Tumor-associated macrophages. Curr Biol 2020;30:R246-8.
26. Reinfeld BI, Madden MZ, Wolf MM, et al. Cell-programmed nutrient partitioning in the tumour microenvironment. Nature 2021;593:282-8.
27. Jeong H, Kim S, Hong BJ, et al. Tumor-Associated Macrophages Enhance Tumor Hypoxia and Aerobic Glycolysis. Cancer Res 2019;79:795-806.
28. Dancsok AR, Gao D, Lee AF, et al. Tumor-associated macrophages and macrophage-related immune checkpoint expression in sarcomas. Oncoimmunology 2020;9:1747340.
29. Surov A, Meyer HJ, Höhn AK, Winter K, Sabri O, Purz S. Associations Between [18F]FDG-PET and Complex Histopathological Parameters Including Tumor Cell Count and Expression of KI 67, EGFR, VEGF, HIF-1α, and p53 in Head and Neck Squamous Cell Carcinoma. Mol Imaging Biol 2019;21:368-74.
30. Surov A, Meyer HJ, Schob S, et al. Parameters of simultaneous 18F-FDG-PET/MRI predict tumor stage and several histopathological features in uterine cervical cancer. Oncotarget 2017;8:28285-96.
31. Lim HJ, Johnny Ong CA, Tan JW, et al. Utility of positron emission tomography/computed tomography (PET/CT) imaging in the evaluation of sarcomas: A systematic review. Crit Rev Oncol Hematol 2019;143:1-13.
32. Murakami W, Tozaki M, Sasaki M, et al. Correlation between (18)F-FDG uptake on PET/MRI and the level of tumor-infiltrating lymphocytes (TILs) in triple-negative and HER2-positive breast cancer. Eur J Radiol 2020;123:108773.
33. Hua T, Zhou W, Zhou Z, et al. Heterogeneous parameters based on (18)F-FET PET imaging can non-invasively predict tumor grade and isocitrate dehydrogenase gene 1 mutation in untreated gliomas. Quant Imaging Med Surg 2021;11:317-27.
34. Li R, Lin J, Wang L, et al. The association between 18F-fluorodeoxyglucose PET intratumoral metabolic heterogeneity and pathological parameters in non-small cell lung cancer. Nucl Med Commun 2019;40:1022-8.

Cite this article as: Chen B, Tao J, Wu T, Feng H, Xie J, Zhong L, Wang S. Correlation between ^{18}F-FDG PET-derived parameters and quantitative pathological characteristics of soft tissue sarcoma. Quant Imaging Med Surg 2023;13(12):7842-7853. doi: 10.21037/qims-23-412

